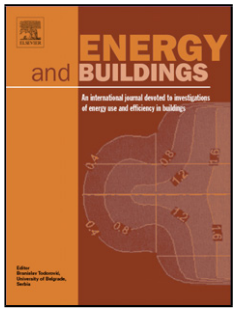

Title: On the error of calculation of heat gains through walls by methods using constant decrement factor and time lag values

Authors: C.R. Ruivo, P.M. Ferreira, D.C. Vaz

PII: S0378-7788(13)00067-4
DOI: doi:10.1016/j.enbuild.2013.02.001
Reference: ENB 4110

To appear in: *ENB*

Received date: 19-6-2012
Revised date: 26-11-2012
Accepted date: 1-2-2013

Please cite this article as: C.R. Ruivo, P.M. Ferreira, D.C. Vaz, On the error of calculation of heat gains through walls by methods using constant decrement factor and time lag values, *Energy and Buildings* (2010), doi:10.1016/j.enbuild.2013.02.001

On the error of calculation of heat gains through walls by methods using constant decrement factor and time lag values

C.R. Ruivo[a,b,*], P.M. Ferreira[d], D.C. Vaz[c,d]

[a]*Departamento de Engenharia Mecânica, Instituto Superior de Engenharia, Universidade do Algarve, Campus da Penha, 8005-139 Faro, Portugal*

[b]*ADAI-LAETA, Departamento de Engenharia Mecânica, Universidade de Coimbra, Rua Luís Reis Santos, 3030-788 Coimbra, Portugal*

[c]*UNIDEMI,* [d]*Departamento de Engenharia Mecânica e Industrial, Faculdade de Ciências e Tecnologia, Universidade Nova de Lisboa, 2829-516 Caparica, Portugal*

Highlights
Numerical simulation of thermal behaviour of external walls of buildings
Evaluation of the decrement factor and time lags of external walls
Evaluation of total equivalent temperature difference
The generalized use of the tested approaches is questionable

Abstract

A transient heat transfer model was developed to numerically predict the thermal behaviour of the external walls of a room under realistic outdoor conditions. The excitation is not simply sinusoidal even though it is considered to have daily periodicity. The numerical model is based on the finite difference method and handles one-dimensional heat conduction through multilayered walls. The boundary condition at the outer surface of the wall is described with the sol-air temperature concept. The

* Corresponding author. Tel.: +351 289 800100; fax: +351 289 888405; e-mail: cruivo@ualg.pt

temperatures of indoor air and of other internal surfaces in the room are assumed to be equal and constant.

The numerical results were used to calculate values of the decrement factor and time lag of several walls. The calculation followed two methods found in literature, in which these parameters are assumed constant, distinguished by the temperature evolution used: the sol-air or the wall's outer surface. Additionally, the inner surface temperature is used in both methods. The walls investigated range from low to high mass construction, face towards various directions and have light or dark coloured sunlit outer surfaces.

The heat fluxes at the inner surface of the walls predicted by numerical modelling and estimated by the simplified methods are compared in detail to conclude on the validity of these simplified methods. As a by-product it is also possible to conclude on the dependence of the decrement factor and of the time lag on the outer surface colour and on the orientation of different types of walls. The results show that both simplified methods have poor accuracy in a significant number of cases. Also, it was found that the wall's azimuth significantly affects the time lag.

Keywords: Multilayer wall, Transient heat transfer, Decrement factor, Time lag

Nomenclature

$CLTD$	Cooling load temperature difference (ºC)
c	Specific heat of building material (J $kg^{-1}ºC^{-1}$)
HC	Heat capacity of the wall per unit area (J $m^{-2}ºC^{-1}$)
h_{ext}	External heat transfer coefficient combining convection and long-wave radiation (W $m^{-2}ºC^{-1}$)

h_{int}	Internal heat transfer coefficient combining convection and long-wave radiation (W $m^{-2}{}^{o}C^{-1}$)
I_t	Total incident solar radiation flux at the outer surface of the wall (W m^{-2})
k	Thermal conductivity of building material (W $m^{-1}{}^{o}C^{-1}$)
L	Thickness of the wall (m)
L_i	Thickness of layer i (m)
M	Mass of the wall per unit of area (kg m^{-2})
n	Number of layers in the wall (W m^{-2})
$\dot{q}_{cond}$	Heat flux by conduction (W m^{-2})
$\dot{q}_{ext}$	Heat flux at the exterior surface of the wall (W m^{-2})
$\dot{q}_{int}$	Heat flux at the interior surface of the wall
R	Thermal resistance ($m^{2}{}^{o}CW^{-1}$)
$SHGF$	Solar heat gain factor for sunlit glass (W m^{-2})
T	Temperature (ºC)
T_{ext}	Outdoor air temperature (ºC)
$\overline{T}_{ext}$	Daily average of outdoor air temperature (ºC)
T_{int}	Indoor air temperature (ºC)
$TETD$	Total equivalent temperature difference (ºC)
T_{sa}	Sol-air temperature (ºC)
t	Time (s)
t_{lag}	Time lag (s)
U	Overall heat transfer coefficient of the wall (W $m^{-2}{}^{o}C^{-1}$)
U_c	Thermal conductance of the wall (W $m^{-2}{}^{o}C^{-1}$)

x	Spatial coordinate, transversal to the wall (m)

Greek symbols

α	Absorptivity of the outer surface of the wall
α_T	Parameter defining the hourly evolution of the outdoor air temperature
β	Admittance of the wall ($W^2\ m^{-4}ºC^{-2}$)
ΔT_{ext}	Daily range of outdoor air temperature (ºC)
δR	Difference between the long-wave radiation flux from sky and surroundings incident on the surface and the radiation flux emitted by a blackbody at the outdoor air temperature ($W\ m^{-2}$)
ε	Hemispherical emissivity of the outer surface of the wall
θ	Azimuth of the wall (º)
ρ	Density of building material ($kg\ m^{-3}$)
Φ	Generic variable representing either the sol-air temperature or the inner or outer surface temperature of the wall
μ	Decrement factor

Subscripts

i , j	Layer number

Abreviations

TFM	Transfer Function Method
TETD/TA	Total Equivalent Temperature Difference/ Time Averaging
XPS	Extruded polystyrene

1. Introduction

The analysis of the heat and mass transfer phenomena in a room is important for: envelope optimization, sizing of the air conditioning system, evaluation of energy consumption, thermal comfort analysis and assessment of occurrence of condensation phenomena on the envelope. The complexity of the actual physical phenomena in buildings and the large uncertainties in the data input required for the evaluation of the cooling and heating loads [1] demand for the use of simple calculation procedures with low computational costs.

Since radiation and convection at both faces of the envelope and the heat gains inside the room are variable in time, the actual thermal behaviour of the room must be predicted by a transient model. During the propagation of the heat wave through a wall, the attenuation of its amplitude depends on the material and thickness of the different layers of the wall. The time period necessary for the heat wave propagate from the outer to the inner surfaces of the wall is named time lag. The ratio between the heat wave amplitudes at the two surfaces of the wall is named decrement factor, respectively. Both parameters are relevant characteristics of a wall because they determine its heat storage capabilities [2].

Accurate methods such as numerical and transfer function methods [3] can be used to determine the thermal load associated with the heat transferred through an external envelope. The transfer function method (TFM) requires the knowledge of transfer functions such as those available for a representative set of roofs and walls [3, 4]. The TFM method is a quite user-friendly approach. When the transfer functions for a particular wall are not found in literature, the problem has to be solved by conducting experimental or numerical simulations, based on finite difference or finite elements methods.

Numerical and transfer function methods are not suitable in the situations that call for a prompt evaluation of the thermal load based on simplified calculations. For actual constructions, this can be addressed with the well-known cooling temperature difference (CLTD) method [3-5] but only if an equivalent construction with known *CLTD* values is identified in the list of reference constructions. A few works have been conducted in order to extend the application of the CLTD method to a vast range of actual constructions in different countries. Bansal *et al.* [6] developed a numerical model, using the finite difference method with an implicit scheme, to simulate the transient thermal behaviour of multilayer walls and roofs of buildings located in Kolkata, India. Marginal to considerable differences are found when comparing the numerically predicted *CLTD* values with those given by the ASHRAE methodology [5]. In other studies the thermal behaviour of a concrete wall was simulated with an analytical method supported by the complex finite Fourier transform technique [7, 8].

One of the first simplified methods developed for the calculation of thermal load across an envelope, the TETD/TA procedure, performs a time averaging (TA) of the total equivalent temperature difference (*TETD*) values to produce an attenuation and a lag in the conversion of heat gain to cooling load. The values of *TETD* can be easily determined by the simplified methods previously mentioned, which use the concepts of sol-air temperature, time lag and decrement factor [9, 10]. The decrement factor and the time lag have been investigated in recent works [11-13]. Both parameters and the simplified methods using them are discussed in more detailed in section 3.

Other research found that both parameters depend on the thickness and position of the insulation layer [14] and on the absorptivity of the outer surface of the envelope [15]. The CIBSE Guide A5 [16] includes an extensive list of decrement factor and time lag

values for walls, which, however, do not take into account the dependence on the wall's azimuth.

The simplified methods using the concepts of decrement factor and time lag [9, 10] are accurate for predicting the *TETD* values for cases with constant indoor air temperature, if the sol-air temperature follows an evolution that is exactly or, at least, very close to sinusoidal.

In spite of the significant number of works carried out [11-15], some misleading concepts [11,12] and doubts [13,14] exist in the literature in what concerns definitions and the use of the decrement factor and the time lag enabling the estimation of *TETD* values. Examples of such unclear problem formulation involving the use of the decrement factor and time lag in simplified methods are mentioned in section 3.4. Moreover, according to the best knowledge of the authors, no research was conducted to inspect in detail the validity of these simplified methods, for the actual cases in which the temperature of the outer side of the wall does not perfectly follow a sinusoidal evolution, since it is imposed by the combined effect of the outdoor air and incident radiation flux evolutions. These are the cases that an engineer finds in practice when performing cooling load calculations.

In the present work, the results obtained by simplified methods based on the decrement factor and time lag are compared against numerical predictions of the thermal behaviour of various walls in order to assess the validity of those simplified methods. In particular, the influence of the orientation of the wall on the decrement factor and the time lag as well as on the *TETD* values is investigated.

The numerical model adopted as reference source takes into account the typical properties and parameters usually considered in thermal load calculations. Its complexity is relatively low due to the assumptions taken into account. It simulates the

unsteady and one dimensional diffusive heat transfer problem. The authors recognize the importance of comparing the predicted results against specific experimental data. However, the undertaking of this experimental work is out of the scope of the present paper. In spite of that, the doubts and misleading concepts encountered in literature about the use of simplified methods based on time lag and decrement factor have motivate the authors in doing this paper towards a better scientific and technical understanding by the community of engineers that usually perform thermal analysis of buildings.

2. Problem formulation

2.1 Analytical model

The simulation of the thermal behaviour of an external multilayer wall is relatively complex due to the transient and three-dimensional nature of the heat and mass transfer phenomena. Fig. 1 illustrates the simplified physical problem for a wall construction, with n layers of different materials. The physical model adopted considers one-dimensional heat flux, similarly to the models that have been used by other authors [6, 11-15, 17]. The most important assumptions are: (*i*) heat conduction takes place along the x direction with no internal heat sources or sinks present, (*ii*) the properties of building materials are constant, (*iii*) the superficial temperatures of other elements such as walls, floors, ceiling, furniture are assumed to be equal to the constant indoor air temperature, (*iv*) the combined surface heat transfer coefficients that account for both convection with the ambient air and radiation with the surrounding surfaces are constant, (*v*) the thermal contact resistance between adjacent material layers is negligible, (*vi*) the mass transfer through the material layers is negligible, (*vii*) the external surface of the envelope is completely dry and in contact with outdoor air, (*viii*)

there is no water vapour condensation on the inner surface of the envelope, (*ix*) the daily evolutions of outdoor air temperature and solar radiation do not change during the period of simulation. This set of assumption is usually considered when a simplified method of calculation of thermal loads is adopted.

The periodic variation on the external conditions cause the heat fluxes at both the inner and outer surface of the wall to vary cyclically, even in the case of constant indoor air temperature (T_{int}). Each layer i of the wall is characterised by: thickness L_i, thermal conductivity k_i, specific heat c_i, and density ρ_i. In the internal domain of each layer the governing equation is:

$$\rho_i c_i \frac{\partial T}{\partial t} + \frac{\partial}{\partial x}\left(-k_i \frac{\partial T}{\partial x} \right) = 0, \tag{1}$$

where $T(x,t)$ is the temperature field and t is time.

Considering perfect thermal contact between two adjacent layers (i and $i+1$), the heat balance at the interface ($x = x_i$ with $x_i = \sum_{j=1}^{i} L_j$ and L_j being the thickness of layer j) leads to:

$$-k_i \left.\frac{\partial T}{\partial x}\right|_{x=x_i^-} = -k_{i+1} \left.\frac{\partial T}{\partial x}\right|_{x=x_i^+}. \tag{2}$$

Convection and long-wave radiation heat transfer occur at the outer surface ($x = 0$) and also in the inner surface ($x = L$) and can be described with combined heat transfer coefficients, h_{ext} and h_{int}, respectively. Then, the heat balances at these surfaces provide two additional equations:

$$\dot{q}_{\text{ext}} = h_{\text{ext}} \left(T_{\text{sa}} - T_{x=0} \right) = -k_1 \left.\frac{\partial T}{\partial x}\right|_{x=0^+}, \tag{3}$$

and

$$\dot{q}_{\text{int}} = h_{\text{int}}\left(T_{x=L} - T_{\text{int}}\right) = -k_n \left.\frac{\partial T}{\partial x}\right|_{x=L^-}, \tag{4}$$

The temperatures of the inner and outer surfaces of the wall are $T_{x=L}$ and $T_{x=0}$, respectively. The sol-air temperature, T_{sa}, can be obtained by [5]:

$$T_{\text{sa}} = T_{\text{ext}} + \frac{\alpha I_{\text{t}}}{h_{\text{ext}}} - \frac{\varepsilon \delta R}{h_{\text{ext}}}, \tag{5}$$

where T_{ext} is the outdoor air temperature, α is the absortivity of the outer surface, I_{t} is the total incident solar radiation flux on the surface, ε is the hemispherical emissivity of the surface and δR is the difference between the long-wave radiation from the sky and surroundings incident on the surface and the radiation emitted by a blackbody at the temperature of outdoor air. In case of vertical constructions, it is common practice to consider $h_{\text{ext}} = 17\ \text{W m}^{-2}\text{ºC}^{-1}$ and $\varepsilon \delta R = 0\ \text{W m}^{-2}$ [5]. As is generally accepted, the cyclical evolution of the outdoor air temperature can be described by:

$$T_{\text{ext}} = \overline{T}_{\text{ext}} - a_{\text{T}} \Delta T_{\text{ext}}, \tag{6}$$

where $\overline{T}_{\text{ext}}$ and ΔT_{ext} are the daily average and the daily range of outdoor air temperature, respectively. The daily evolution of the parameter a_{T} depends on the latitude and on the day. Table 1 presents hourly values of a_{T} for a place at a latitude of 40ºN, in July.

In Eq. (5), the total solar radiation, I_{t}, is also assumed to vary periodically. It could be predicted through a specific physical model [6, 8], but since I_{t} on an outer surface is the same be it a glass or a wall, it is predicted in the present work simply by:

$$I_{\text{t}} = SHGF / 0.87. \tag{7}$$

where $SHGF$ is the solar heat gain factor, available in table form [5], for the sunlit double-strength sheet glass (DSA), 3 mm in thickness. The value 0.87 is the solar heat

gain coefficient for the same glass [5]. The cases investigated in the present paper are always within the range covered by this table [5]. The hourly values of $SHGF$, obtained from the clear-sky model [5] and usually used for calculating the heat gains through fenestration, are considered and linearly interpolated in each hour period to better describe the time evolution.

The location of the insulation layer, the overall coefficient of heat transfer (U), the thermal conductance (U_c), the mass (M) and the heat capacity (HC) referred to a 1 m^2 area of transfer surface are also important characteristic data of the wall. Those parameters can be obtained from the following equations:

$$U = \left(\frac{1}{h_{\text{ext}}} + \sum_{i=1}^{n} \frac{L_i}{k_i} + \frac{1}{h_{\text{int}}} \right)^{-1}, \tag{8}$$

$$U_c = \left(\sum_{i=1}^{n} \frac{L_i}{k_i} \right)^{-1}, \tag{9}$$

$$M = \sum_{i=1}^{n} \rho_i L_i , \tag{10}$$

and

$$HC = \sum_{i=1}^{n} \rho_i c_i L_i , \tag{11}$$

The total equivalent temperature difference ($TETD$) can be predicted through:

$$TETD = \frac{\dot{q}_{\text{int}}}{U} . \tag{12}$$

2.2 Numerical solution

It is difficult to analytically solve the present physical problem. Therefore, a numerical approach is followed to solve Eq. (1) together with the boundary and initial conditions. The finite difference method is adopted, supported by the explicit formulation. The numerical tool was developed by Ferreira [17] to analyse the dynamic thermal

behaviour of walls with and without phase change materials. Ferreira [17] conducted a deep mesh independence study considering a wall composed by a layer of concrete and a layer of insulation. The study of Ferreira [17] shows that the criteria adopted in defining the number of nodes in each material layer and the time step provides: (i) good results for walls incorporating phase change material (uncertainty of about 2%) and (ii) excellent results in case of walls without phase change materials (negligible uncertainty), which is the case investigated in the present manuscript.

The code was implemented in MATLAB and a user-friendly tool was developed, which easily provides the values of total equivalent temperature differences, decrement factor and time lag for multilayered walls.

3 Simplified methods based on decrement factor and time lag

3.1 Decrement factor and time lag

The decrement factor and the time lag have been presented and interpreted as parameters relating the evolutions of two variables Φ_{ext} and Φ_{int}, as illustrated in Fig. 2. In researches [2, 15, 18] it is clear that the problem is presented considering $\Phi_{\text{ext}} = T_{x=0}$ and $\Phi_{\text{int}} = T_{x=L}$. This case is also adopted in the present investigation as well as the case considering $\Phi_{\text{ext}} = T_{\text{sa}}$ and $\Phi_{\text{int}} = T_{x=L}$.

The wall's decrement factor and time lag have been presented as:

$$\mu = \frac{\Delta\Phi_{\text{int}}}{\Delta\Phi_{\text{ext}}} = \frac{\Phi_{\text{int,max}} - \Phi_{\text{int,min}}}{\Phi_{\text{ext,max}} - \Phi_{\text{ext,min}}}, \tag{13}$$

and

$$t_{\text{lag}} = t_{\Phi_{\text{int,max}}} - t_{\Phi_{\text{ext,max}}}, \tag{14}$$

respectively, just using the amplitudes of both variables and the instants when their maximum and minimum values are observed.

3.2 Two simplified methods

Mackey and Wright [9] have recognized that few engineers will care to use a method as complete as the one they developed. Furthermore, they state that the use of a simple enough approximate method is preferred since it warrants general use without too great sacrifice in the accuracy of the final result.

The heat flux at the inner surface of a wall can be estimated at each instant in a simplified way by:

$$\dot{q}_{\text{int}}^{*} = U \times TETD\,, \tag{15}$$

where $TETD$ represents the instantaneous total equivalent temperature difference, which must take into account the different dynamic effects affecting the transient behaviour of the wall.

In the present work two different approaches of obtaining $TETD$ daily evolutions are investigated. One of them is supported by the well known formula [7,8,19,20]:

$$TETD_{1} = \overline{T}_{\text{sa}} - T_{\text{int}} + \mu_{1}\left(T_{\text{sa}}^{\text{lag1}} - \overline{T}_{\text{sa}}\right), \tag{16}$$

and is here designated by method M1. The variable $T_{\text{sa}}^{\text{lag1}}$ is the sol-air temperature at instant $t - t_{\text{lag1}}$, $\overline{T}_{\text{sa}}$ is its daily average value and T_{int} is the indoor air temperature.

Another method, M2, is the simplest approximate solution presented by Mackey and Wright [9]. It begins by predicting the instantaneous temperature of the inner surface of the wall from:

$$T_{x=L} = \overline{T}_{x=L} + \mu_{2}\left(T_{\text{sa}}^{\text{lag2}} - \overline{T}_{\text{sa}}\right), \tag{17}$$

where the mean daily temperature of the inner surface of the wall is estimated by the steady-state solution:

$$\overline{T}_{x=L} = T_{\text{int}} + \frac{U}{h_{\text{int}}}\left(\overline{T}_{\text{sa}} - T_{\text{int}}\right), \tag{18}$$

Manipulating Eqs. (4), (17) and (18), the *TETD* value at instant t can be estimated by:

$$TETD_2 = \overline{T}_{sa} - T_{int} + \mu_2 \frac{h_{int}}{U}\left(T_{sa}^{lag2} - \overline{T}_{sa}\right) . \quad (19)$$

For the application of method M2, the values of μ_2 and t_{lag2} for an actual wall can be read from graphics developed for homogeneous walls [9] by taking into account the properties of the corresponding equivalent homogeneous construction [10].

According to Eqs. (16) and (19), the decrement factors μ_1 and μ_2 of a particular wall are imperatively different and the following relationship holds:

$$\mu_1 = \mu_2 \, h_{int}/U . \quad (20)$$

The underlying assumption $t_{lag1} = t_{lag2}$, which is equivalent to consider that the sol-air temperature and the outer surface temperature of the wall reach the maximum values at the same instant. In fact this should be the case since the outer surface of a wall is immaterial, that is, it has no associated mass.

This is depicted in Fig. 3 considering $h_{int} = 8.29 \text{ W m}^{-2}\text{°C}^{-1}$ and $h_{ext} = 17 \text{ W m}^{-2}\text{°C}^{-1}$. The line with $U = 5.57 \text{ W m}^{-2}\text{°C}^{-1}$ corresponds to a wall with infinite thermal conductance ($U_c = +\infty$).

In both approaches, M1 and M2, the decrement factors are close to 0 for walls with very low thermal conductance [9]. For the case of a very thin wall with negligible thermal conductive resistance and negligible mass, the time lag is insignificant as well as the attenuation of the heat transfer imposed by the wall. Under these conditions the *TETD* values are estimated simply by the difference between T_{sa} and T_{int} and the decrement factors assume a maximum value that depends on the approach used. In method M1, the maximum decrement factor is $\mu_1 = 1$ [19, 20] and in method M2 it is $\mu_2 = 0.672$, a

value that was estimated by Eq. (20) ($\mu_2 = \mu_1 U/h_{\text{int}}$) with $h_{\text{int}} = 8.29\ \text{W m}^{-2}\text{°C}^{-1}$, $h_{\text{ext}} = 17\ \text{W m}^{-2}\text{°C}^{-1}$ and $U = \left(1/h_{\text{int}} + 1/h_{\text{ext}}\right)^{-1}$.

The parameters μ_2 and t_{lag2} were first investigated for homogeneous walls and roofs, and their dependence on the admittance and thermal conductance of the envelope was graphically represented [9]. As an extension of this work [9], a conversion procedure of a composite construction to an equivalent homogeneous construction was presented, as well as a set of rather unwieldy equations enabling the determination of μ_2 and t_{lag2} for two- and three-layer constructions [10].

3.3 Analysis of two walls of Mackey and Wright through method M2

Two of the constructions investigated by Mackey and Wright [10], walls numbers 31 and 32, are analysed in the present work. Both walls are composed of three layers ($n = 3$). Table 2 gives, for both walls, values of thermal resistance $R = L/k$ and admittance $\beta = \rho k c_{\text{p}}$ of each layer. Table 3 gives the values of thermal conductance U_{c} and overall coefficient U. The pair of variables $\mu_{2\text{A}}$ and t_{lag2A} listed in the same table was predicted with precise equations by Mackey and Wright [10] and the other pair $\mu_{2\text{B}}$ and t_{lag2B} were estimated from the graphical information after calculation of the parameters β and U_{c} for an equivalent homogenous construction [9,10]. The overall heat transfer coefficient was calculated considering the following values assumed by Mackey and Wright [9]: $h_{\text{int}} = 4.0\ \text{Btu h}^{-1}\text{ft}^{-2}\text{F}^{-1}$ and $h_{\text{ext}} = 1.65\ \text{Btu h}^{-1}\text{ft}^{-2}\text{F}^{-1}$, or in SI units, $h_{\text{ext}} = 22.7\ \text{W m}^{-2}\text{°C}^{-1}$ and $h_{\text{int}} = 9.37\ \text{W m}^{-2}\text{°C}^{-1}$.

For the case study of the two walls facing south, with dark outer surface, on July and at latitude 40ºN, *TETD* values were predicted by method M2, considering $\overline{T}_{ext}$ =28.3 ºC and ΔT_{ext} =11.7 ºC.

Fig. 4 depicts the solutions obtained with the pair (μ_{2A} , t_{lag2A}), labelled SA, and with the pair (μ_{2B}, t_{lag2B}), labelled SB. In both cases, the indoor air temperature is $T_{int} = 25\ ^{\circ}C$. It is observed that, as expected, the differences between both solutions are not negligible and are due to the differences in decrement factors and time lags. This disagreement between solutions justifies additional investigations to be carried out to evaluate the accuracy of both solutions SA and SB by comparing them with numerical predictions.

3.4 Assessment of method M1

In what regards the use of method M1, the influences of the wall thickness and the density of the construction material on the decrement factor and on the time lag are presented in [19]. However, the curves presented just allow an approximate estimation of time lag and decrement factor. The more complete set of curves presented in [20] shows the influence of the overall heat transfer coefficient and of the penetration coefficient ($\sqrt{\beta}$) of the wall on μ_1 and t_{lag1}. This graphical information, applicable to method M1, seems to be the equivalent of the graphical data applicable to method M2 [9]. In method M2, the pair (μ_2, t_{lag2}) can be estimated as a function of the thermal conductance and of the admittance of the wall. The CIBSE Guide A5 [16] presents a procedure enabling the calculation of the decrement factor and the time lag values for a set of 38 walls and 26 roofs.

As illustrated in Fig. 2, the evaluation of both the decrement factor and the time lag has been obtained directly from the evolutions of a particular variable (Φ) in the outer and inner side of the wall [11-15].

Kaska *et al.* [12] calculate the decrement factor by Eq. (13). According to the nomenclature of this work it seems that they considered $\Phi_{int} = T_{int}$ and $\Phi_{ext} = T_{ext}$. It should be noted that with this definition, a constant indoor air temperature would lead to a null decrement factor. The outside air temperature (T_{ext}) alone does not represent well the outdoor condition because it neglects the effect of the incident radiation. Moreover, the illustration offered by Kaska *et al.* [12], similar to that presented in Fig. 2, shows periodic evolutions for the sol-air temperature and for the indoor air temperature. The problem is presented in a misleading way and no clue is given on how the decrement factor values were calculated.

The values predicted for the four walls investigated by Kaska *et al.* [12] (nos. 31, 32, 33 and 34) are apparently applicable to method M1 because the values of *TETD* were predicted with Eq. (15). The achieved μ_1 values were compared directly with those derived with precise equations by Mackey and Wright [10], solution SA, not with the approximate solution SB obtained with method M2 [9]. The μ_1 values predicted in [12] are greater than the μ_2 values, in accordance to Fig. 3. However, the differences in the range of 11% to 30% are not corroborated by the data of Fig. 3. The application of Fig. 3, as a graphical representation of Eq. (20), to convert the predicted μ_1 values into μ_2 values, applicable to method M2, would lead to differences of around 90%.

Even though this relation has not been confirmed, the *TETD* evolutions predicted by Kaska *et al.* [12] agree well with those obtained using the data of Mackey and Wright [10]. Further investigation is required to obtain an explanation for the results achieved.

In another research of Kaşka and Yumrutaş [11], the illustration of the problem does not agree with the description in the text, but it is explicitly referred that the variables Φ_{int} and Φ_{ext} correspond to the inner and outer surface temperatures of the wall. This assumption does not make sense when the *TETD* values are estimated by method M2. In fact, the maximum decrement factor obtained from the evolutions $\Phi_{\text{ext}} = T_{x=0}$ and $\Phi_{\text{int}} = T_{x=L}$ is μ=1 when the wall presents negligible conductive thermal resistance and negligible mass. In turn, when using the method M2 the maximum value of the decrement factor is $\mu_2 = 0.672$, according to the section 3.2.

However, the *TETD* values predicted by the method M1 closely match those obtained by Mackey and Wright [10] under similar conditions. The problem is clearly presented in [15,2,18], but doubts persist in the works [13,14,21]. Reference [14] would be clearer if in the illustration of the problem the temperature of the outer surface had been used instead of the represented evolution of the sol-air temperature.

The illustration of the problem presented in [20] shows that $\Phi_{\text{ext}} = T_{\text{ext}}$ and $\Phi_{\text{int}} = T_{\text{int}}$. The estimation of decrement factor and time lag based on this assumption is unreasonable because the effect of the incident radiation on the outer surface is not taken into account and the indoor temperature is constant.

4. Results and discussion

The heat flux $\dot{q}_{\text{int}}$ predicted by numerical modelling and the heat flux $\dot{q}^*_{\text{int}}$ estimated by the simplified methods are compared in detail to conclude on the dependence of the decrement factor and of the time lag on the outer surface colour and on the orientation of different types of walls. In particular, the analysis is performed by comparing the estimated $TETD^*$ and the predicted *TETD* values. Table 4 specifies the set of 6

multilayered walls and the set of 4 monolayer walls analysed in the present study. The walls are low to high mass constructions and are simulated when facing north, east, south and west. The simulations are performed for a place at a latitude of approximately 40ºN with summer sunny day weather conditions for the month of July. The daily average temperature ($\overline{T}_{\text{ext}}$) is 28.3 ºC and the daily range of outdoor air temperature (ΔT_{ext}) is 17.1 ºC. Light coloured ($\alpha = 0.44$) and dark coloured ($\alpha = 0.88$) sunlit walls are investigated. The assumed indoor air temperature is $T_{\text{int}} = 25\ ^{\circ}\text{C}$.

The daily evolutions of the sol-air temperature are calculated by Eq. (5) for each orientation and each colour of the outer surface. These evolutions are illustrated in Fig. 5 for the case of dark coloured surface, and a deviation relatively to the sinusoidal pattern can be observed.

The present study also addresses the differences between the results predicted while considering the real evolutions of the sol-air temperature (see Fig. 5) and those predicted while assuming the sinusoidal in the form:

$$T_{\text{sa}}(t) = \frac{T_{\text{sa,min}} + T_{\text{sa,max}}}{2} - \sin\left(\frac{2\pi t}{24 \times 3600}\right)\frac{T_{\text{sa,max}} - T_{\text{sa,min}}}{2}, \tag{24}$$

with t in seconds. Fig. 6 depicts two evolutions of the sol-air temperature, SIN1 and SIN2, in which the maximum values assumed are $T_{\text{sa,max}} = 77.22\,^{\circ}\text{C}$ and $T_{\text{sa,max}} = 52.96\,^{\circ}\text{C}$, respectively. In both cases it was assumed $T_{\text{sa,min}} = 19.7\,^{\circ}\text{C}$.

4.1 A monolayer wall

The properties of the monolayer wall W10 are those of the coating of the multilayered walls. The predicted evolutions of the temperatures and heat fluxes at the outer and inner surfaces are represented in Fig. 7 for the dark coloured wall W10 facing south.

Table 5 lists for wall W10 facing north, east, south, and west, for both light and dark colour, the decrement factors and time lags derived from the numerical results and from

the two additional sinusoidal evolutions of T_{sa}. It is observed that these sinusoidal evolutions do not affect both the decrement factor and the time lag. This contrasts with the real case in which both parameters depend on the orientation and on the colour of the outer surface of the wall. The values of the ratio μ_1/μ_2 are in complete disagreement with those of the ratio h_{int}/U indicated in Table 5. From this inspection it seems that the use of method M1 leads to important errors in the estimation of *TETD* hourly values.

When using method M2, the decrement factor and the time lag can be determined by the graphical inspection presented by Mackey and Wright in [9]. When using method M1, the methodology presented in [20] can be pursued.

After the calculation of the penetration coefficient and of the overall coefficient of the wall W10 ($\sqrt{\beta} = 59.35\ \mathrm{kJ\,m^{-2}\,^oC^{-1}h^{-0.5}}$ and $U = 3.155\ \mathrm{W\,m^{-2}\,^oC^{-1}}$) the time lag and the decrement factor to be used in method M1 [20] are approximately $\mu_1 = 0.92$ and $t_{lag1} = 2\,\mathrm{h}$). After the calculation of the admittance and of the thermal conductance of the wall W10 ($\beta = 8.43\ \mathrm{Btu^2\,h^{-1}ft^{-4}F^{-2}}$ and $U_c = 0.61\ \mathrm{Btu\,h^{-1}ft^{-2}F^{-1}}$) the time lag and the decrement factor to be used in method M2 [9] are approximately $\mu_2 = 0.32$ and $t_{lag2} = 2.2\,\mathrm{h}$. Both simplified approaches used to find these values do not take into account both the orientation and the colour of the outer surface of the wall.

The above values of μ_2 and t_{lag2} refer to cases with $h_{ext} = 22.7\ \mathrm{W\,m^{-2}\,^oC^{-1}}$ and $h_{int} = 9.37\ \mathrm{W\,m^{-2}\,^oC^{-1}}$. So, their direct comparison with the values listed in Table 5 is not strictly correct. Consequently, wall W10 was again simulated considering the above values of h_{ext} and h_{int} adopted in [9]. The results are indicated in Table 6 and show that the decrement factor μ_2 ranges between 0.301 and 0.338, which is due to the

influence of the orientation and of the colour of the wall. That interval contains the value $\mu_2 = 0.32$, indicated above The time lag t_{lag2} varies from 1.82 to 2.78 and also compares well with $t_{lag2} = 2.2\,\text{h}$. So, this indicates that method M2 provides reasonably accurate results when estimating the heat flux $\dot{q}_{int}$ or the corresponding *TETD* daily evolution of wall W10. This good agreement is also corroborated by the values predicted for both sinusoidal evolutions SIN1 and SIN2. For an example when considering the sinusoidal evolution SIN1, a relative difference of 0.04% is observed between the peak value of *TETD* estimated by method M2 with μ_1=0.333 and t_{lag1}=2.5 h and the peak predicted by the numerical model.

A strong disagreement between the values of μ_1 in Table 5 and $\mu_1 = 0.92$ is observed, relative differences are about 110%, leading also to the conclusion that important errors in the evaluation of *TETD* values by method M1 are expected with $\mu_1 = 0.92$ when $\Phi_{ext} = T_{x=0}$ and $\Phi_{int} = T_{x=L}$. As an example, the peak value of *TETD* predicted by method M1 considering the sinusoidal evolution SIN1 with $\mu_1 = 0.92$ and $t_{lag1} = 2\,\text{h}$ is 38% greater than the peak value predicted by the same method with μ_1=0.445 and t_{lag1}=1.62 h.

The *TETD* values predicted by the model and estimated by methods M1 and M2 are depicted in Figs. 8 and 9 for the dark coloured W10 wall facing south and east, respectively. As expected, the largest deviation is observed between the evolution predicted by the model and the evolution estimated by method M1.

4.2 A multilayer wall

Table 7 lists the decrement factors and time lags calculated from the numerical results for the wall construction W5 facing north, east, south, and west, and light and dark

coloured. Figs. 10 to 12 refer to the dark coloured wall W5. From Fig. 10 it can be observed that the heat flux at the inner surface of the wall facing south is quite constant throughout the day due to the fairly constant evolution of the inner surface temperature. The *TETD* values estimated by method M1 that are depicted in both Figs. 11 and 12 evidence an appreciable disagreement against those predicted by the numerical model. The relative errors between peak *TETD* values are about 36% and 25% for the dark coloured wall W5 facing south and east, respectively.

The results provided by method M2 show a reasonable agreement when applied to walls facing south (see Fig. 11), but according to the trends depicted in Fig. 12 important errors can be involved when using this simplified method. The relative errors between peak *TETD* values are about 13% and 17% for the dark coloured wall W5 facing south and east, respectively.

An explanation for these errors may be that T_{sa} does not follow an exact sinusoidal evolution, an important subject that should be investigate in further research.

4.3 Error in the *TETD* evolutions estimated by simplified methods

To quantify the deviation between the *TETD* evolution predicted by the numerical model and the $TETD^*$ evolution estimated by one of the simplified methods (M1 and M2), we define the following error indicator:

$$\sigma_i = \frac{1}{TETD_{\max}} \sqrt{\frac{1}{24} \sum_{j=1}^{24} \left(TETD(j) - TETD_i^*(j) \right)^2} \quad . \tag{25}$$

where $i = \text{M1, M2}$ and $TETD_{\max}$ is the maximum value of the evolution predicted by the numerical model.

Table 8 presents the values of the error indicator for both walls W5 and W10. Fig. 13 summarizes the results of the error indicator obtained with the approaches M1 and M2, for the set of 80 cases investigated. In the great majority of cases it is observed that

$\sigma_{M2} < \sigma_{M1}$ and hence according to the error indicator (Eq. (25)) method M2 better estimates the $TETD$ evolution. However, method M2 only provides good accuracy (error lower than 5%) in a third of the cases. When using method M1 the error indicator is higher than 8.3% for all the cases investigated.

Due to the underlying simplifying hypotheses, the numerical model is not exact. However, the physical problem to be solved is simple in nature and its implementation in the code is relatively simple. Therefore, the numerical model was taken as the reference when extracting the required indicators for analysis. Another alternative to the use of the developed model would be resorting to dynamic simulation programs, such as EnergyPlus or TRNSYS.

4.4 Influence of the azimuth on the time lag and decrement factor for the wall W5

An additional set of simulations of the dark coloured wall W5 was conducted with the wall facing N, NNE, NE, ENE, SE, SSE, S, SSW, SW, WSW, W, WNW, NW and NNW to examine the dependence of the time lag and of the decrement factor on the azimuth of the wall, θ. Fig. 14 depicts the results for those parameters associated to the method M2. It is observed that the azimuth has a small influence on the decrement factor $\mu_2(\theta)$ and an appreciable influence on $t_{lag2}(\theta)$: the difference between the maximum and minimum values is about 8 h. This also sustains the need for improving the simplified methods to extend their use to a large range of wall constructions at an arbitrary orientation.

To the best of the authors' knowledge, the validity of the use of simplified methods based on time lag and decrement factor has not been thoroughly investigated. Method M2 provides accurate results when the daily evolutions of sol-air temperature are sinusoidal, which is not the case in real situations, especially when the wall is not due south. The deviations between sol-air temperature evolutions and the perfect sinusoidal

evolution influence the accuracy of the results provided by those methods. The percentage of cases with poor accuracy is significant and hence, the use of these simplified approaches is questionable.

5. Conclusions

A numerical model solving the daily periodic behaviour of a building external wall was formulated and used in the simulation of a large set of light and dark coloured walls facing north, east, south and west. Two simplified methods were tested to evaluate the heat flux at the inner surface, or the *TETD* evolutions, by using the sol-air temperature concept, the decrement factor and the time lag. When using the decrement factor estimated by the ratio between the daily ranges of the inner and outer surfaces temperatures, the simplified method produces results that are not accurate. When using the decrement factor estimated by the ratio between the daily ranges of inner surface temperature and the sol-air temperature the accuracy of the results is significantly improved. However, the improvement is not enough to extend the use of the method to a large range of wall constructions at an arbitrary orientation *because the azimuth of the wall significantly affects the time lag*. The deviations of sol-air temperature evolutions from perfect sinusoidal evolutions influence the accuracy of the results obtained with the simplified methods. The percentage of cases with poor accuracy is significant. Therefore, the generalized use of the simplified approaches published in the literature is questionable and further research should be conducted to investigate on the derivation of appropriate correlations for the correction of the decrement factor and time lag parameters.

References

[1] F. Domínguez-Muñoz, J.M. Cejudo-López, A. Carrillo-Andrés, Uncertainty in peak cooling load calculations, Energy Build. 42 (7) (2010) 1010–1018.

[2] H. Asan, Numerical computation of time lags and decrement factors for different building materials, Build. Environ. 41 (5) (2006) 615–620.

[3] ASHRAE handbook – Fundamentals. Atlanta: ASHRAE; 1993.

[4] McQuiston FC, Parker JD. Heating, ventilating, and air conditioning. 4th ed. New York: Wiley; 1994.

[5] ASHRAE handbook – Fundamentals. Atlanta: ASHRAE; 1989.

[6] K. Bansal, S. Chowdhury, M.R. Gopal, Development of CLTD values for buildings located in Kolkata, Appl. Therm. Eng. 28 (10) (2008) 1127–1137.

[7] R. Yumrutaş, M. Ünsal, M. Kanoğlu, Periodic solution of transient heat flow through multilayer walls and flat roofs by complex finite Fourier transform technique, Build. Environ. 40 (8) (2005) 1117–1125.

[8] Ö. Kaşka, R. Yumrutaş, Comparison of experimental and theoretical results for the transient heat flow through multilayer walls and flat roofs, Energy 33 (12) (2008) 1816–1823.

[9] C. Mackey, L. Wright, Periodic heat flow-homogeneous walls or roofs, ASHVE Transactions 50 (1944); 293–312.

[10] C. Mackey, L. Wright, Periodic heat flow-composite walls or roofs, ASHVE Transactions 52 (1946); 283–296.

[11] Ö. Kaşka, R. Yumrutaş, Experimental investigation for total equivalent temperature difference (TETD) values of building walls and flat roofs, Energy Convers. Mgmt. 50 (11) (2009) 2818–2825.

[12] Ö. Kaska, R. Yumrutaş, E. Yıldırım, Estimation of total equivalent temperature difference values for multilayer walls and flat roofs by using periodic solution, Build. Environ. 42 (5) (2007) 1787–1885.

[13] Ö. Kaska, R. Yumrutaş, O. Arpa, Theoretical and experimental investigation of total equivalent temperature difference (TETD) values for building walls and flat roofs in Turkey, Appl. Energy 86 (5) (2009) 737–747.

[14] H. Asan, Effects of wall's insulation thickness and position on time lag and decrement factor, Energy Build. 28 (3) (1998) 299–305.

[15] K.J. Kontoleon, D.K. Bikas, The effect of south wall's outdoor absorption coefficient on time lag, decrement factor and temperature variations, Energy Build. 39 (9) (2007) 1011–1018.

[16] Environmental Design CIBSE Guide A, CIBSE, The Yale Press Ltd., London, 2006.

[17] P. Ferreira, Comportamento térmico dinâmico dos elementos da envolvente opaca de edifícios: com estudo de incorporação de materiais com mudança de fase, Master Thesis, Universidade Nova de Lisboa, Lisboa, Portugal, 2011.

[18] K.J. Kontoleon, E.A. Eumorfopoulou, The influence of wall orientation and exterior surface solar absorptivity on time lag and decrement factor in the Greek region, Renewable Energy 33 (7) (2008) 1652–1664.

[19] W.P. Jones, 7 – Heat Gains from Solar and Other Sources, Air Conditioning Engineering, 5th ed. 2001. 144–215 doi: org/10.1016/B978-075065074-8/50009-8

[20] Recknagel, Sprenger, Hönmann. Manual Técnico de Calefacción y Aire Acondicionado, Tomo II Aire Acondicionado y Frio, Belisco Ediciones Técnicas y Científicas, 1st ed. Madrid, 2001.

[21] K. Ulgen, Experimental and theoretical investigation of the effects of wall's thermophysical properties on time lag and decrement factor, Energy Build. 34 (3) (2002) 273–278.

Table 1 – Hourly values of the parameter a_T.

Solar time t (h)	1	2	3	4	5	6	7	8
a_T	0.31	0.39	0.45	0.49	0.50	0.48	0.40	0.29
Solar time t (h)	9	10	11	12	13	14	15	16
a_T	0.15	0.00	-0.15	-0.29	-0.40	-0.48	-0.50	-0.49
Solar time t (h)	17	18	19	20	21	22	23	24
a_T	-0.45	-0.39	-0.31	-0.22	-0.11	0.00	0.11	0.22

Table 2 – Thermal resistance and admittance of layers of walls nos. 31 and 32 [10]

Property	Layer i	Wall no. 31	Wall no. 32
R ($m^2\,°C\,W^{-1}$)	Layer 1	0.044	0.11
	Layer 2	0.107	0.213
	Layer 3	0.107	0.427
β ($W^2m^{-4}°C^{-2}$)	Layer 1	5.68×10^5	5.68×10^5
	Layer 2	6.04×10^5	6.04×10^5
	Layer 3	6.04×10^5	6.04×10^5

Table 3 – Overall properties of walls nos. 31 and 32 [10]

Property	Wall no. 31	Wall no. 32
β ($W^2m^{-4}{}^oC^{-2}$)	11.2×10^5	11.3×10^5
U_c ($Wm^{-2}{}^oC^{-1}$)	3.88	1.33
U ($Wm^{-2}{}^oC^{-1}$)	2.45	1.11
μ_{2A}	0.2142	0.0219
t_{lag2A} (h)	3.38	12.2
μ_{2B}	0.16	0.009
t_{lag2B} (h)	5.5	17

Table 4 – Description of wall constructions (L_i (m); ρ_i (kg m^{-3}); k_i (W m^{-1}ºC^{-1}); c_i (J kg^{-1}ºC^{-1}); U (W m^{-2}ºC^{-1}); M (kg m^{-2}); HC (J m^{-2} ºC^{-1})

Wall	**Layer** i	**Material**	L_i	ρ_i	k_i	c_i	U	M	HC $\times 10^{-3}$	h_{int}/U
W1	1	Ext. coating	0.01	1602	0.727	840	0.776	33	280	10.68
	2	XPS insulation	0.04	30	0.037	1210				
	3	Int. coating	0.01	1602	0.727	840				
W2	1	Ext. coating	0.01	1602	0.727	840	2.928	100	84	2.83
	2	Common brick	0.07	965	0.520	840				
	3	Int. coating	0.01	1602	0.727	840				
W3	1	Ext. coating	0.01	1602	0.727	840	1.454	273	230	5.70
	2	Common brick	0.25	965	0.520	840				
	3	Int. coating	0.01	1602	0.727	840				
W4	1	Ext. coating	0.01	1602	0.727	840	1.690	225	189	4.91
	2	Common brick	0.20	965	0.520	840				
	3	Int. coating	0.01	1602	0.727	840				
W5	1	Ext. coating	0.02	1602	0.727	840	0.575	278	234	14.42
	2	Common brick	0.11	965	0.520	840				
	3	XPS insulation	0.04	30	0.037	1210				
	4	Common brick	0.11	965	0.520	840				
	5	Int. coating	0.02	1602	0.727	840				
W6	1	Ext. coating	0.02	1602	0.727	840	0.480	451	380	17.27
	2	Common brick	0.20	965	0.520	840				
	3	XPS insulation	0.04	30	0.037	1210				
	4	Common brick	0.20	965	0.520	840				
	5	Int. coating	0.02	1602	0.727	840				
W7	1	Insulation	0.05	91	0.043	840	0.745	5	4	11.13
W8	1	Concrete	0.10	2243	1.731	840	4.215	224	188	1.97
W9	1	Concrete	0.30	2243	1.731	840	2.835	673	565	2.92
W10	1	Monolayer	0.10	1602	0.727	840	3.155	160	135	2.63

Table 5 – Time lag, decrement factor and ratios μ_1/μ_2 predicted for wall W10

		t_{lag1} (h)	t_{lag2} (h)	μ_1	μ_2	μ_1/μ_2
Dark coloured	North	2.56	3.48	0.447	0.340	1.31
	East	1.66	2.71	0.421	0.292	1.44
	South	1.72	1.99	0.435	0.320	1.36
	West	1.22	2.00	0.431	0.313	1.38
Light coloured	North	2.18	3.10	0.446	0.337	1.32
	East	1.73	2.22	0.425	0.300	1.42
	South	1.63	2.59	0.438	0.322	1.36
	West	1.32	1.98	0.435	0.319	1.36
Sinusoidal evolutions of T_{sa}	SIN1	1.62	2.5	0.445	0.333	1.33
	SIN2	1.62	2.5	0.445	0.333	1.33

Table 6 – Time lag and decrement factor predicted for a W10 wall with the values of h_{ext} and h_{int} used in ref. [9]

		t_{lag1} (h)	t_{lag2} (h)	μ_1	μ_2	μ_1/μ_2
Dark coloured	North	2.10	2.78	0.419	0.338	1.24
	East	1.63	2.67	0.397	0.301	1.32
	South	1.70	1.98	0.410	0.323	1.27
	West	1.38	1.86	0.407	0.318	1.28
Light coloured	North	2.18	3.10	0.446	0.337	1.32
	East	1.73	2.22	0.425	0.300	1.42
	South	1.63	2.63	0.413	0.327	1.26
	West	1.45	1.82	0.410	0.324	1.27
Sinusoidal evolutions of T_{sa}	SIN1	1.50	2.30	0.418	0.333	1.25
	SIN2	1.50	2.30	0.418	0.333	1.25

Table 7 – Time lag, decrement factor and ratios μ_1/μ_2 predicted for wall W5

		t_{lag1} (h)	t_{lag2} (h)	μ_1	μ_2	μ_1/μ_2
Dark coloured	North	7.46	8.60	0.034	0.028	1.21
	East	11.36	11.37	0.028	0.021	1.33
	South	8.38	8.73	0.033	0.026	1.26
	West	5.96	6.85	0.029	0.023	1.26
Light coloured	North	7.56	8.72	0.034	0.028	1.22
	East	12.02	12.53	0.033	0.025	1.32
	South	8.64	9.66	0.034	0.027	1.26
	West	6.32	7.10	0.030	0.024	1.25

Table 8 – Error indicator values for walls W5 and W10

		Wall W10		Wall W5	
		σ_{M2}	σ_{M1}	σ_{M2}	σ_{M1}
Dark coloured	North	0.045	0.244	0.065	0.191
	East	0.187	0.222	0.106	0.151
	South	0.081	0.254	0.053	0.181
	West	0.130	0.252	0.056	0.169
Light coloured	North	0.037	0.266	0.058	0.202
	East	0.243	0.225	0.085	0.194
	South	0.113	0.270	0.058	0.200
	West	0.125	0.266	0.052	0.183

Figure Captions

Fig. 1. Heat transfer in a wall with n layers.

Fig. 2. Cyclic behaviour of a wall.

Fig. 3. Relationship between the decrement factors of both methods M1 and M2.

Fig. 4. Predicted *TETD* values for walls nos. 31 and 32 [10].

Fig. 5. Sol-air temperature evolutions for dark coloured surfaces facing different directions.

Fig. 6. Two sinusoidal evolutions of sol-air temperature differing in the maximum value.

Fig. 7. Temperature and heat flux evolutions at the outer and the inner surfaces of a dark coloured W10 wall facing south.

Fig. 8. Evolutions of *TETD* for dark coloured W10 wall and facing south.

Fig. 9. Evolutions of *TETD* for dark coloured W10 wall and facing east.

Fig. 10. Temperature and heat flux evolutions at outer and inner surfaces of wall W5 with dark coloured and facing south.

Fig. 11. Evolutions of *TETD* for wall W5 with dark coloured and facing south.

Fig. 12. Evolutions of *TETD* for wall W5 facing east and dark coloured.

Fig. 13. Error indicators σ_{M2} and σ_{M1} for the set of 80 cases investigated.

Fig. 14. Dependence of both time lag and decrement factor on the azimuth of the dark coloured wall W5.

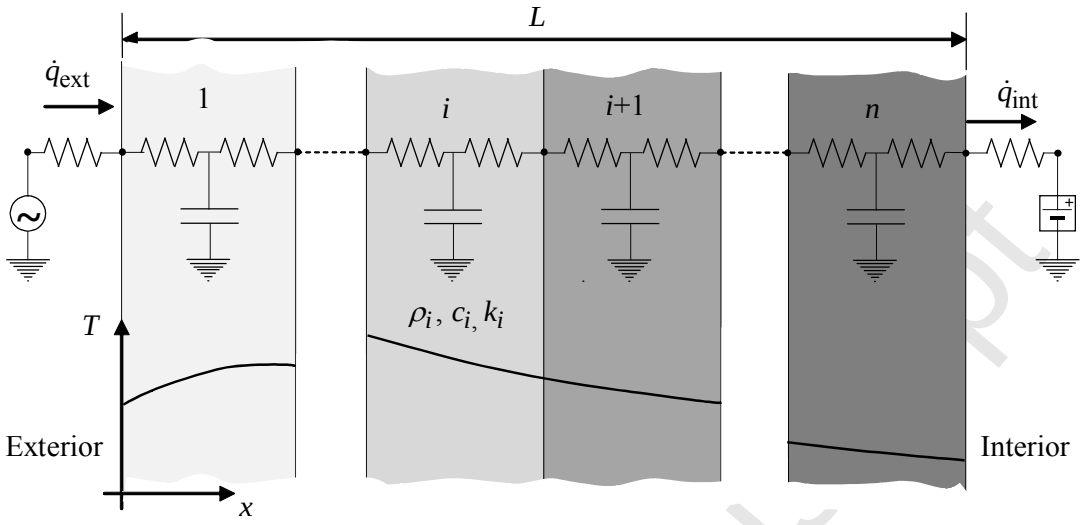

Fig. 1.

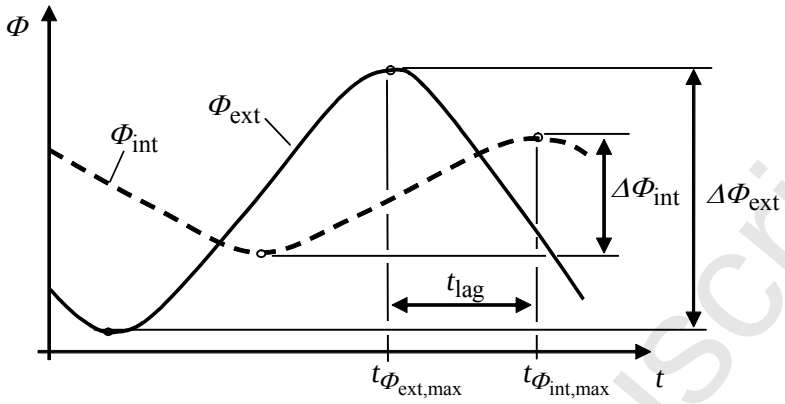

Fig. 2.

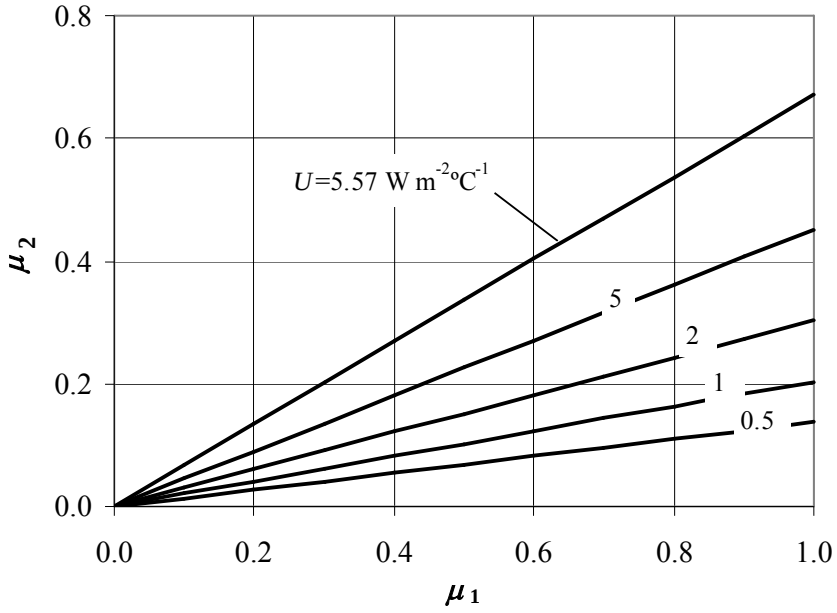

Fig. 3

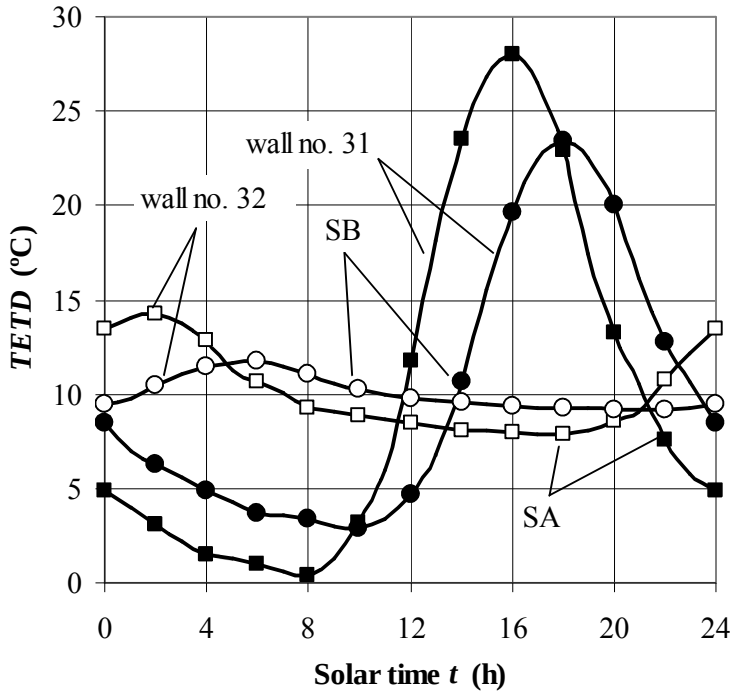

Fig. 4

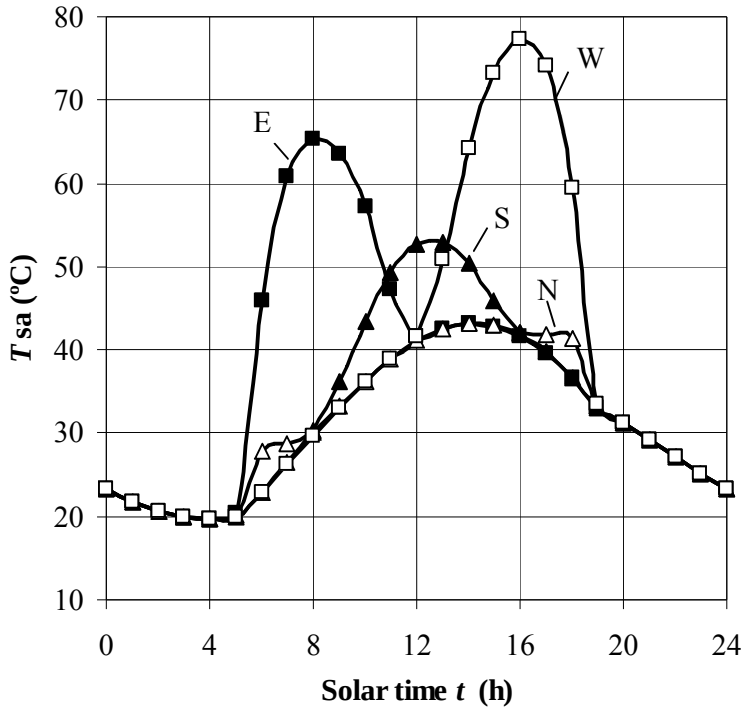

Fig. 5.

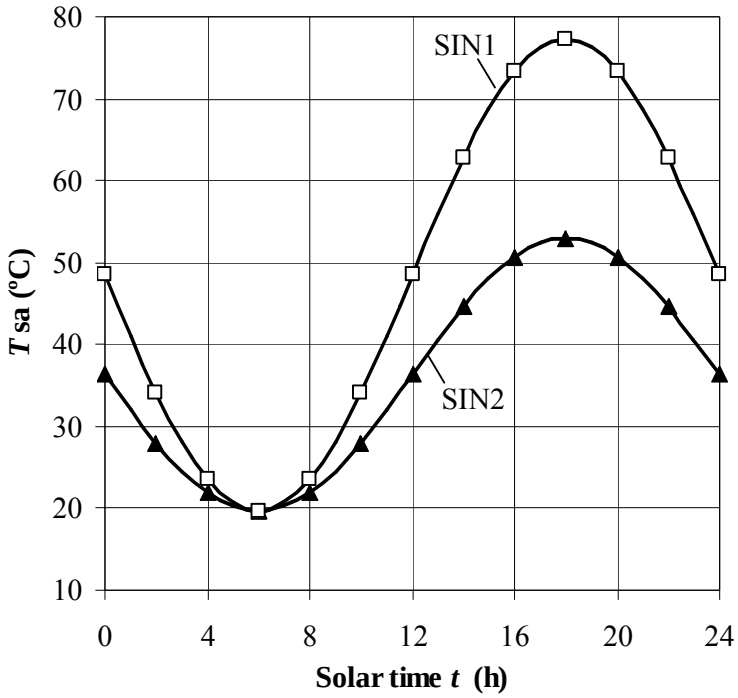

Fig. 6.

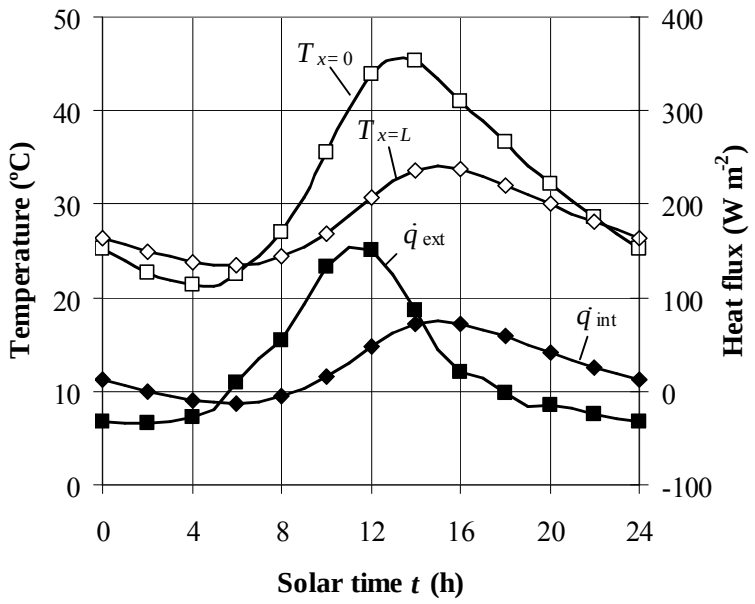

Fig. 7.

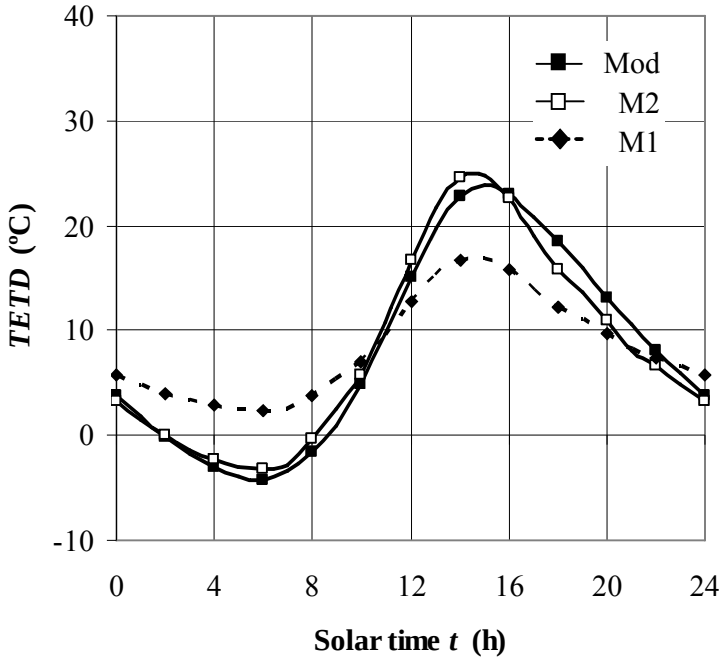

Fig. 8

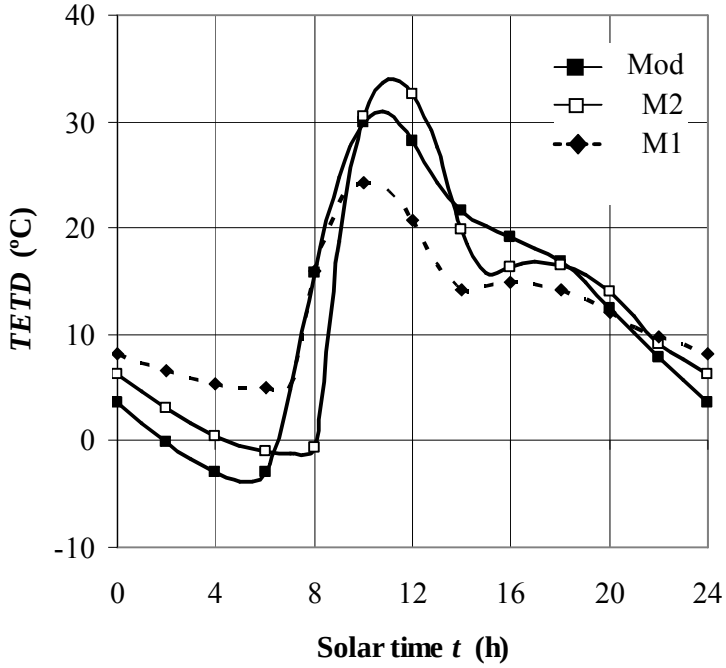

Fig. 9

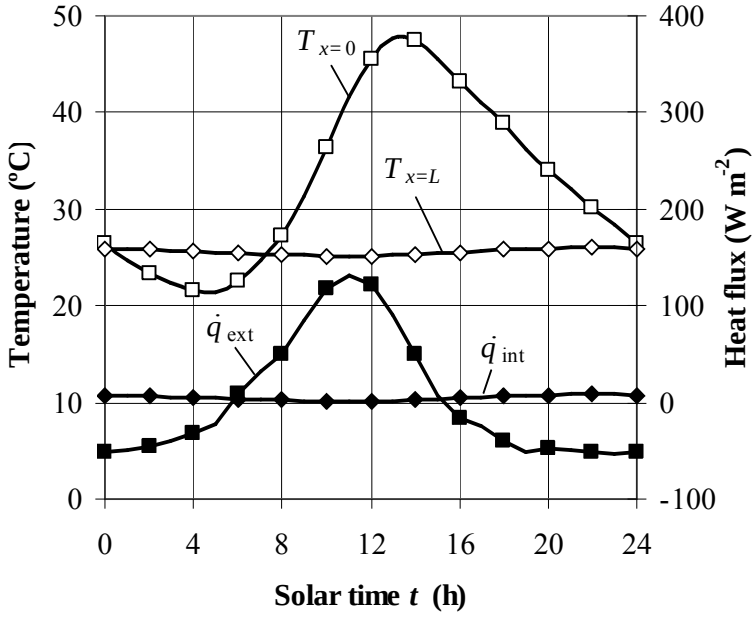

Fig. 10.

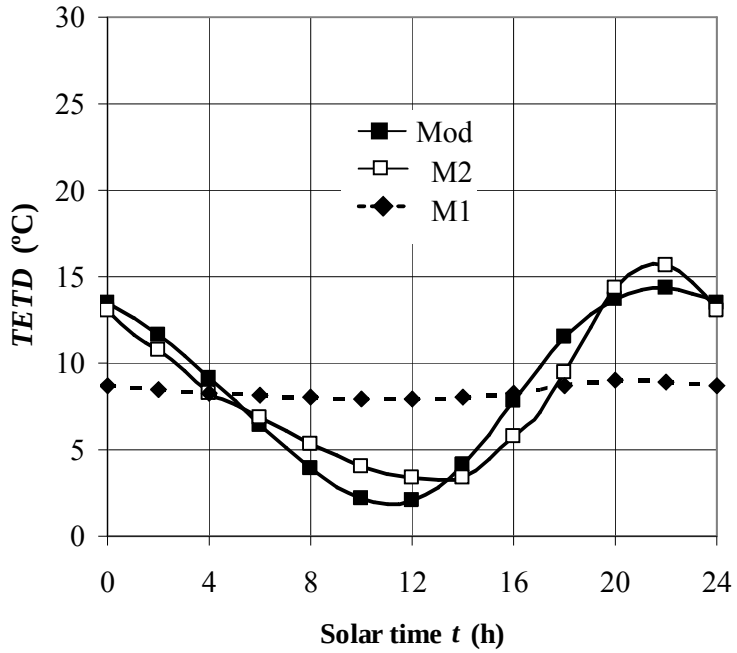

Fig. 11

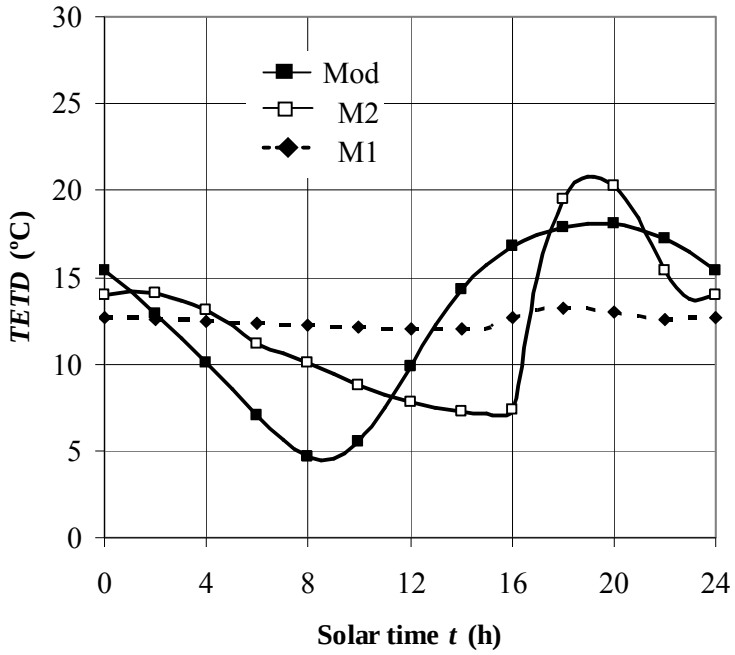

Fig. 12.

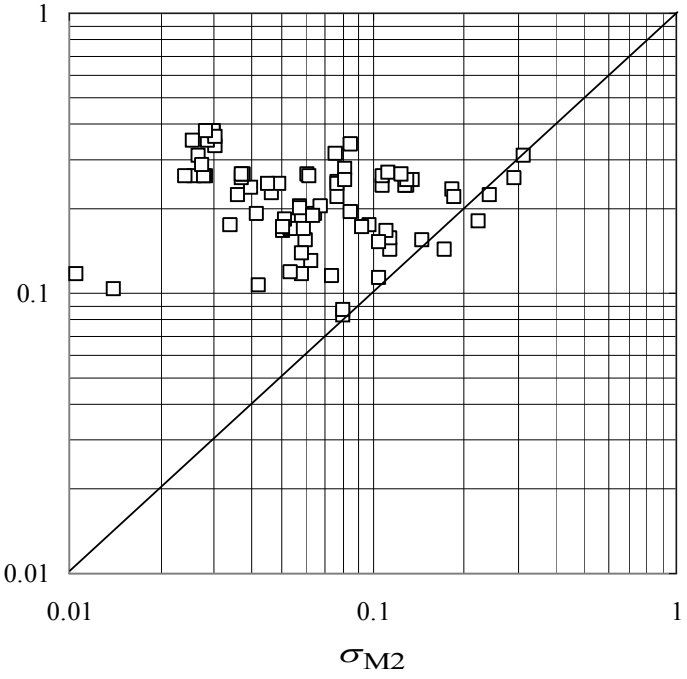

Fig. 13.

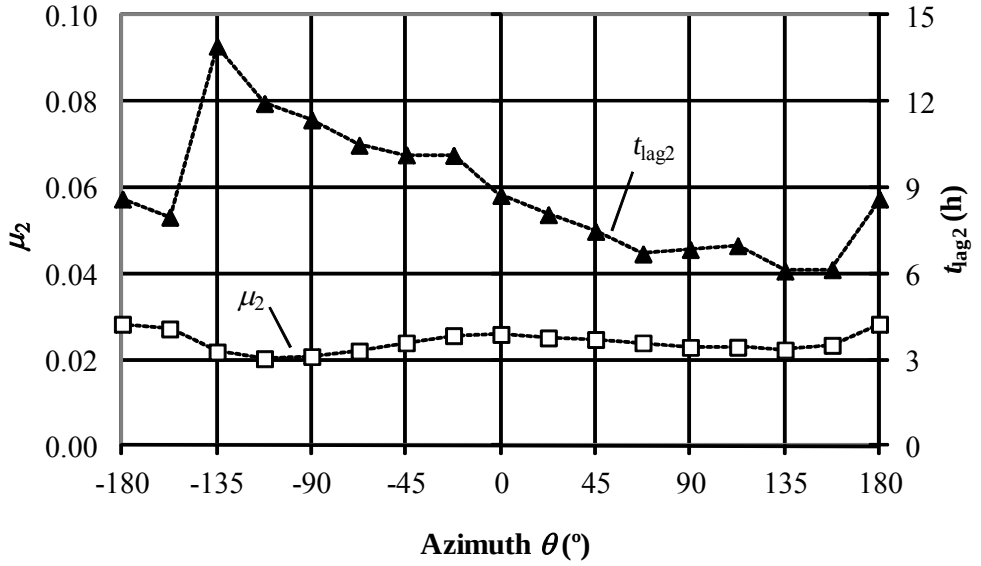

Fig. 14.